

Nucleosynthesis in multidimensional simulations of SNI

C. Travaglio^a, K. Kifonidis^a, E. Müller^a

^a*Max-Planck Institut für Astrophysik, Karl-Schwarzschild Strasse 1, D-85741 Garching bei München, Germany*

Abstract

We investigate explosive nuclear burning in core collapse supernovae by coupling a tracer particle method to one and two-dimensional Eulerian hydrodynamic calculations. Adopting the most recent experimental and theoretical nuclear data, we compute the nucleosynthetic yields for $15 M_{\odot}$ stars with solar metallicity, by post-processing the temperature and density history of advected tracer particles. We compare our results to 1D calculations published in the literature.

Key words: stars: late stages of evolution, nucleosynthesis, supernovae: nucleosynthesis

PACS: 97.60, 97.10.C, 26.20, 26.30, 95.30.C

1 Introduction

The pre- and post-explosive nucleosynthesis of massive stars has been studied extensively by several groups over the last years (see Woosley & Weaver 1995; Thielemann et al. 1996; Limongi et al. 2000; Rauscher et al. 2002, and the references therein). Although a lot of work has been performed in this field, computed nucleosynthetic yields are still affected by numerous uncertainties. For instance, because of our rather sketchy current understanding of the physical mechanism(s) that lead from core collapse to supernovae (SNe), all studies of explosive nucleosynthesis, that have been performed to date, made use of ad hoc energy deposition schemes to trigger SN explosions in progenitor models. While the results of such calculations indicate that the yields of only a rather small number of nuclei are sensitive to the details of how the supernova shock is launched (see e.g. Woosley&Weaver 1995), it is nevertheless important to attempt to compute nucleosynthetic yields in the framework of more sophisticated models of the explosion. The impact of multidimensional hydrodynamics has not been investigated in detail so far. In addition, among the

isotopes whose yields are known to depend sensitively on the explosion mechanism, and thus cannot be predicted accurately at present, are key nuclei, like ^{56}Ni and ^{44}Ti , that are of crucial importance for the evolution of supernova remnants and for the chemical evolution of galaxies. These nuclei have also important consequences for numerical supernova models. Their yields can be used as a sensitive probe for the conditions prevailing in SNe and hence can serve to constrain hydrodynamic SN models with their complex interdependence of neutrino-matter interactions, multi-dimensional hydrodynamic effects, as well as the explosion mechanism itself.

2 Hydrodynamic models

The nucleosynthesis calculations presented in this work are based on one and two-dimensional hydrodynamic models of SNe which follow the revival of the stalling shock, which forms after iron core collapse, and its propagation through the star from 20 ms up to a few seconds after core bounce (when the explosion energy has saturated and all important nuclear reactions have frozen out). The simulations are started from post-collapse models of Rampp & Janka (priv. comm.), who followed core-collapse and bounce in the $15 M_{\odot}$, $Z = Z_{\odot}$ progenitors of Woosley & Weaver (1995) and Limongi et al. (2000). We employ the HERAKLES code, which solves the hydrodynamic equations in 1, 2 or 3 spatial dimensions with the direct Eulerian version of the Piecewise Parabolic Method (Colella & Woodward 1984), and which incorporates the light-bulb neutrino treatment and the equation of state of Janka & Müller (1996) (for more details see Kifonidis et al. 2003, and the references therein). The main advantages of our approach are that we drive the shock by accounting for neutrino-matter interactions in the layers outside the newly born neutron star, instead of using a piston (see e.g. Woosley & Weaver 1995) or a “thermal bomb”, and the possibility to perform calculations from one up to three spatial dimensions.

3 Marker particle method

Choosing a hydrodynamic scheme for computing multi-dimensional hydrodynamic models that include the nucleosynthesis, one faces the dilemma of using either a Lagrangian or an Eulerian method. Since nuclear networks with hundreds of isotopes are prohibitively expensive in terms of CPU time and memory for multi-dimensional calculations, such networks can only be solved in a post-processing step (the energy source term due to nuclear burning can usually be calculated with a small network online with the hydrodynamics,

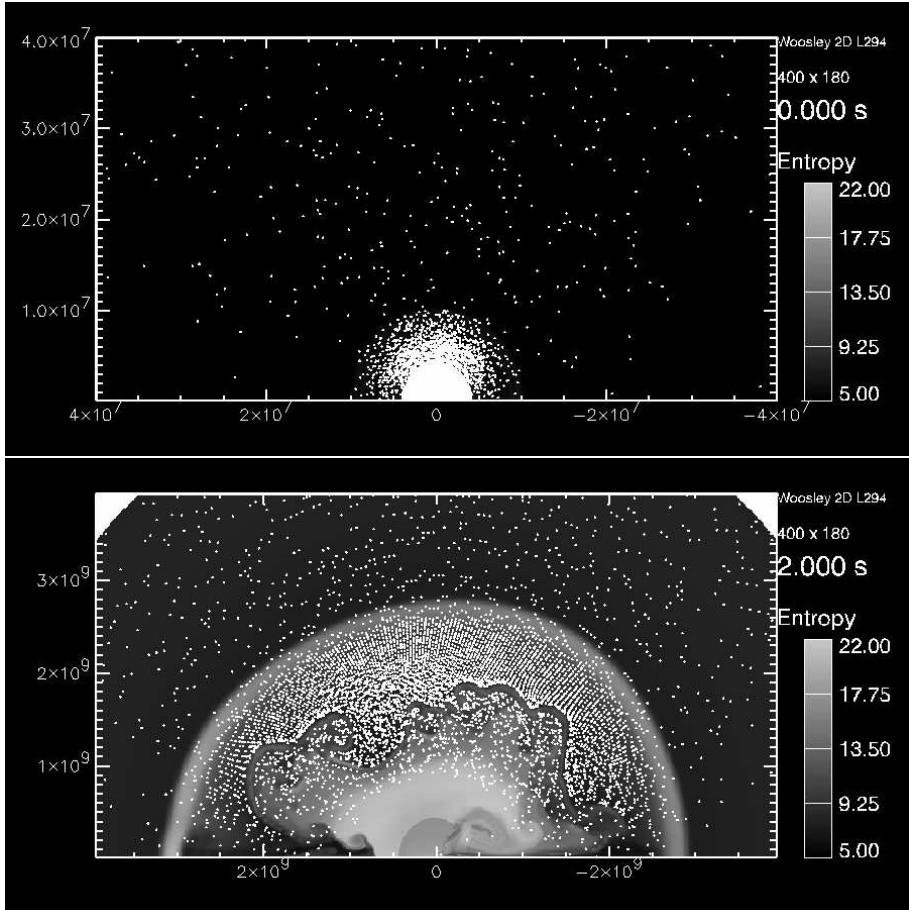


Fig. 1. *Upper panel:* initial marker particle distribution within 400 km of the computational domain of a 2D simulation (model L294). The entropy (in $k_b/\text{nucleon}$) is depicted in the background. *Lower panel:* final marker particle distribution. Note the change of the radial scale, the pile-up of particles in the dense layer between the (light colored) low-density, neutrino-heated bubble, almost void of markers, and the shock farther out.

and may even be neglected completely in some cases, depending on the structure of the progenitor). Using an Eulerian scheme (where the grid is fixed in space) or even adaptive schemes (in which the grid automatically adapts to resolve steep gradients in the solution) the problem arises how one should obtain the necessary data for the post-processing calculations. We do this by adding a “Lagrangian component” to our Eulerian scheme in the form of marker particles that we passively advect with the flow in the course of the Eulerian calculation, recording their T and ρ history by interpolating the corresponding quantities from the underlying Eulerian grid. A similar method has been adopted in a previous study of multi-dimensional nucleosynthesis in core collapse SNe by Nagataki et al. (1997), in very massive stars (Maeda et al. 2002), and in Type Ia SNe (Niemeyer et. al. 2002).

For our 1D and 2D calculations we have used 1024 and 8000 marker par-

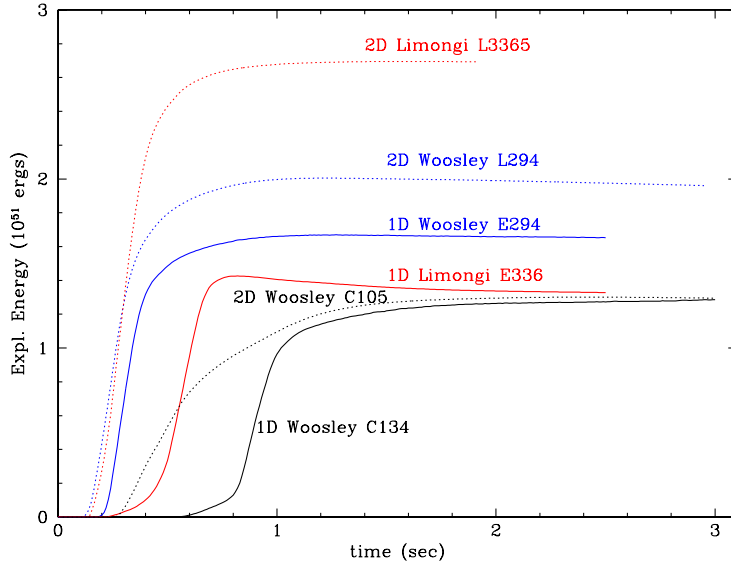


Fig. 2. Explosion energies for the different models discussed in the text.

ticles, respectively. They are distributed homogeneously in mass throughout the progenitor’s Fe core, Si, O, and C shells assuming the composition of the progenitor at the corresponding mass coordinate as the initial composition of the respective tracer particle. Fig. 1 *upper panel* shows the initial distribution of the particles in the innermost region of the computational domain for a 2D simulation that was started from the s15s7b progenitor of Woosley & Weaver (1995). The final distribution of the particles (at a time of 2s after core bounce) is given in Fig. 1 *lower panel* for the same simulation. In both Figures the entropy distribution is plotted in the background. Fig. 1 demonstrates that the particles trace mainly the high-density region of the ejecta (which is located between the shock and the neutrino-heated bubbles), and that still the spatial resolution of the hydrodynamic calculation is not compromised in the low-density, neutrino-heated layers due to the Eulerian nature of our hydrodynamic scheme.

4 Nucleosynthesis: results and perspectives

Given the temperature and density history of individual marker particles we can calculate their nucleosynthetic evolution and compute the total yields (including the decays of unstable isotopes) as a sum over all particles. The reaction network employed for our nucleosynthesis calculations contains 296 nuclear species, from neutrons, protons, and α -particles to ^{78}Ge (F.-K. Thielemann, priv. comm.). The reaction rates include experimental and theoretical nuclear data as well as weak interaction rates.

In order to estimate the effects of the spatial resolution of the hydrodynamic calculations on the nucleosynthetic yields we have performed resolution studies in one spatial dimension. Varying both the number of markers and Eulerian zones, we adjusted the numerical resolution such that errors resulting from interpolation between these two “grids” are less than a few per cent for a simulation with 2000 zones and 1024 marker particles. Keeping the resolution of the Eulerian grid fixed at 2000 zones and varying the number of markers, we obtain convergence of the yields, if the number of particles exceeds ~ 1000 . For 10 times less markers, gradients in the hydrodynamic quantities are not sampled sufficiently accurately, affecting the final composition by $\sim 20\%$. Numerical convergence depends also on the accuracy of the hydrodynamic quantities themselves, i.e. on the resolution of the Eulerian grid. We have not investigated this in detail so far but plan to do this in forthcoming calculations. In addition, the one-dimensional results may not be applicable to the two-dimensional situation. Therefore, a resolution study in two spatial dimensions is also in preparation.

So far we have investigated six explosion models for their nucleosynthetic yields: a one-dimensional (E294) and a corresponding two-dimensional (L294) model that made use of model s15s7b of Woosley & Weaver (1995), with high energy of the explosion. A second pair of a one (E336) and two-dimensional (E3365) simulation for the $15 M_{\odot}$ Limongi et al. (2000) progenitor. Also in this second case the explosion energy obtained is high. Finally, a third pair of a one (C134) and two-dimensional (C105) simulation for the $15 M_{\odot}$ s15s7b of Woosley & Weaver (1995), but with a much lower explosion energy. The properties of these models are given in Table 1, where $L_{\nu_e,52}^0$ is the electron neutrino luminosity (in units of 10^{52} erg/s), $E_{exp,51}$ is the explosion energy (in units of 10^{51} erg), and t_{exp} is the explosion time scale (in ms) defined as the time after the start of the simulation when the explosion energy exceeds 10^{49} erg (for a detailed explanation of the neutrino parameters see Janka & Müller 1996 and Kifonidis et al. 2003). In the last column of Table 1 we also added the ^{56}Ni mass obtained using these hydrodynamic models and the nucleosynthesis calculations described above.

Fig. 2 shows the evolution of the explosion energy for the six models, using the same neutrino luminosity for the 1D and 2D model of the same progenitor. The Limongi et al. (2000) progenitor needs higher neutrino luminosity to explode, mainly due to the fact that it has a more compact core. The C134 and C105 models evolve much slower in time (as an effect of a lower explosion energy. Our goal is to investigate the consequences on nucleosynthesis (in particular mixing can play a major role under these conditions).

In Fig. 3 we compare the yields of the 1D and 2D simulations (E294 and L294, respectively) for the Woosley & Weaver (1995) progenitor. The differences, which are apparently negligible in case of the lighter nuclei and small

Table 1

Parameters of models, using the Woosley&Weaver (1995, WW95) and Limongi et al. (2000, LSC00) progenitors.

Model	Zones	$N_{markers}$	$L_{\nu_e,52}^0$	$E_{exp,51}$	t_{exp} (ms)	^{56}Ni (M_{\odot})
E294	2000	1024	2.940	1.46	230	0.192
L294	400×180	8000	2.940	1.99	125	0.120
E336	2000	1024	3.365	1.33	260	0.234
L3365	400×180	8000	3.365	2.69	150	0.146
C134	2000	1024	1.344	1.28	600	0.085
C105	400×180	8000	1.050	1.29	280	0.064

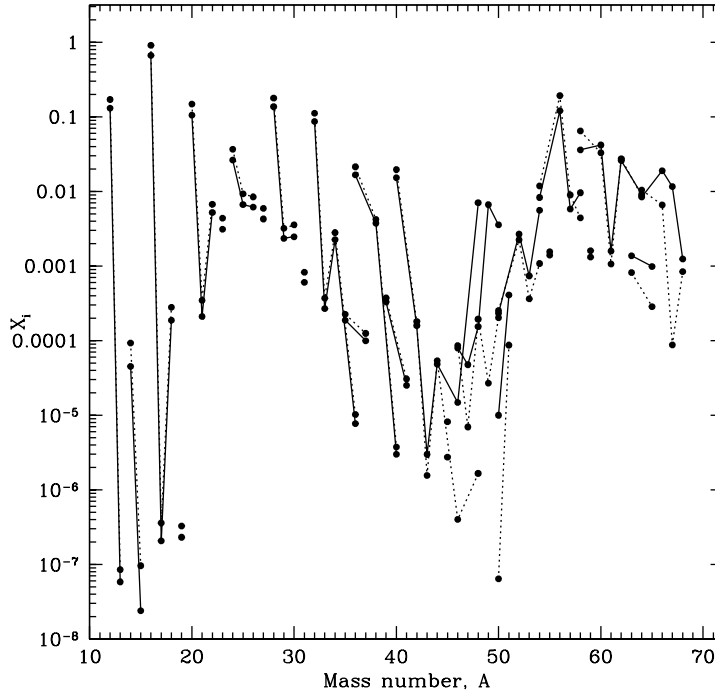


Fig. 3. Final mass fractions obtained for the 1D (*dotted line*) and 2D simulation (*solid line*) as a function of the atomic number, for the cases E294 and L294.

for the heavier ones, are mainly due to the on average higher temperatures in the 2D simulation, i.e. more free neutrons are available in the innermost layers of the 2D simulation. This results in higher production factors for isotopes very sensitive to neutron captures, like e.g. $^{46,48}\text{Ca}$, $^{49,50}\text{Ti}$, $^{50,51}\text{V}$, ^{54}Cr , and ^{67}Zn . In Table 2 we summarize the resulting synthesized masses for the models described above using the Woosley & Weaver (1995) progenitor, and for selected stable as well as radioactive isotopes interesting in the 1D/2D comparison. Note that each column is for a different model as described in

Table 2

Synthesized mass (M_{\odot}) in different SNII models for selected isotopes.

Species	E294	L294	C134	C105
^{12}C	1.7E-01	1.3E-01	8.4E-02	1.2E-01
^{16}O	9.1E-01	6.7E-01	4.4E-01	5.9E-01
$^{22}\text{Na}^r$	7.0E-07	5.0E-07	3.7E-07	5.6E-07
$^{26}\text{Al}^r$	8.4E-06	6.1E-06	3.6E-06	4.6E-06
$^{36}\text{Cl}^r$	2.1E-06	1.9E-06	8.8E-07	8.0E-07
$^{40}\text{K}^r$	6.7E-07	9.1E-07	3.2E-07	6.8E-07
^{40}Ca	2.0E-02	1.5E-02	6.6E-03	1.3E-02
$^{41}\text{Ca}^r$	2.9E-05	2.4E-05	9.4E-06	2.0E-05
^{44}Ca	3.7E-06	5.3E-06	1.8E-06	6.9E-06
^{46}Ca	4.0E-07	1.5E-05	1.9E-07	2.6E-05
$^{44}\text{Ti}^r$	5.0E-05	4.3E-05	2.7E-05	2.3E-05
^{48}Ti	1.5E-06	9.6E-06	7.2E-07	1.9E-05
^{49}Ti	3.0E-06	6.6E-03	7.5E-03	2.3E-03
^{50}Ti	2.0E-04	3.6E-03	8.7E-05	3.2E-03
$^{53}\text{Mn}^r$	3.5E-04	3.1E-04	9.0E-05	2.1E-04
^{54}Fe	1.2E-02	8.3E-03	4.4E-03	5.3E-03
^{56}Fe	6.1E-04	4.0E-03	3.4E-04	2.7E-03
$^{60}\text{Fe}^r$	7.4E-04	5.5E-03	1.5E-04	5.2E-03
$^{57}\text{Ni}^r$	8.8E-03	5.0E-03	3.6E-03	2.3E-03
^{63}Cu	6.1E-04	5.1E-04	2.0E-04	3.1E-04
^{65}Cu	1.8E-04	9.1E-04	9.6E-05	1.5E-03
^{64}Zn	1.0E-02	8.4E-03	2.7E-03	3.5E-03
^{66}Zn	6.1E-03	3.3E-03	2.5E-03	3.4E-03

^(r) – Radioactive

Table 1, and only the mass fractions carried by the tracer particles are included in Table 2. A more detailed discussion on nucleosynthesis calculation in multidimensional simulations of SNII is included in Travaglio et al. (2003, in preparation), where also a network extended to heavier isotopes has been considered.

For the cases with high energy of the explosion, the reason for the rather small differences in the yields between the 1D and 2D simulations are the high initial neutrino luminosities, that we adopted for our calculations, and their rapid exponential decline. This leads to very rapid (and energetic) explosions (Fig. 3). The short explosion time scale prevents the convective bubbles, which form due to the negative entropy gradient in the neutrino-heated region, to merge to large-scale structures that can lead to global anisotropies, and hence to significant differences compared to the 1D case. Lowering the neutrino luminosities (and the explosion energies), as in the cases C134 and C105, we obtain stronger convection that strongly distorts the shock wave by developing large bubbles of neutrino-heated material (see Janka & Müller 1996; Kifonidis et al. 2000 for examples). Adopting constant core luminosities instead of an exponential law, we can produce models where the phase of convective overturn lasts for several turn-over times and which exhibit the vigorous boiling behaviour reported by Burrows et al. (1995). Such cases can finally develop global anisotropies, showing a dominance of the $m = 0$, $l = 1$ mode of convection (see Janka et al. 2003; Scheck et al. 2003). As a consequence, convection can lead to large deviations from spherical symmetry, and thus to larger differences in the final

yields than those visible in Fig. 3. We are currently investigating such models in more detail.

5 Acknowledgements

C.T. thanks the Alexander von Humboldt Foundation, the Federal Ministry of Education and Research, and the Programme for Investment in the Future (ZIP) of the German Government for their financial support.

References

- [14] Burrows, A., Hayes, J., & Fryxell, B. A. (1995), *ApJ*, **450**, 830
- [14] Colella, P., & Woodward, P.R. (1984), *J.Comput.Phys.*, **54**, 174
- [14] Janka, H.-Th., & Müller, E. (1996), *A&A*, **306**, 167
- [14] Janka, H.-Th., Buras, R., Kifonidis, K., Plewa, T., & Rampp, M. (2003), in *From Twilight to Highlight: The Physics of Supernovae*, ed. W. Hillebrandt & B. Leibundgut (Berlin: Springer)
- [14] Kifonidis, K., Plewa, T., Janka, H.-Th., & Müller, E. (2000), *ApJ*, **531**, L123
- [14] Kifonidis, K., Plewa, T., Janka, H.-Th., & Müller, E. (2003), *A&A*, in press
- [14] Limongi, M., Straniero, O., & Chieffi, S. (2000), *ApJS*, **129**, 625
- [14] Maeda, K., Nakamura, T., Nomoto, K., Mazzali, P., Patat, F., & Hachisu, I. (2002), *ApJ*, **565**, 405
- [14] Nagataki, S., Hashimoto, M.-A., Sato, K., & Yamada, S. (1997), *ApJ*, **486**, 1026
- [14] Niemeyer, J., Reinecke, M., Travaglio, C., & Hillebrandt, W. 2002, Workshop "From Twilight to Highlight: The Physics of Supernovae" (2002), p. 151
- [14] Rauscher, T., Heger, A., Hoffman, R.D., & Woosley, S.E. (2002), *ApJ*, **576**, 323
- [14] Scheck, L., Plewa, T., Janka, H.-T., Kifonidis, K., & Müller, E. (2003), astro-ph/0307352
- [14] Thielemann, F.-K., Nomoto, K., & Hashimoto, M.-A. (1996), *ApJ*, **460**, 408
- [14] Woosley, S.E., & Weaver, T.A. (1995), *ApJS*, **101**, 181